Silencing cuticular pigmentation genes enables RNA FISH in intact insect appendages

Accepted manuscript

Pentzold, S., Grabe, V., Ogonkov, A., Schmidt, L., Boland, W., & Burse, A.

Published in: **Journal of Experimental Biology**

Reference:

Pentzold, S., Grabe, V., Ogonkov, A., Schmidt, L., Boland, W., & Burse, A. (2018). Silencing cuticular pigmentation genes enables RNA FISH in intact insect appendages. Journal of Experimental Biology. doi:10.1242/jeb.185710.

Web link: http://dx.doi.org/10.1242/jeb.185710

Contact: Dr. Stefan Pentzold

Department of Bioorganic Chemistry
Max Planck Institute for Chemical Ecology
Beutenberg Campus
Hans-Knoell-Strasse 8
D-07745 Jena
Germany

e-mail: spentzold@ice.mpg.de

First posted online on 19 July 2018 as 10.1242/jeb.185710
Access the most recent version at http://jeb.biologists.org/lookup/doi/10.1242/jeb.185710

Silencing cuticular pigmentation genes enables RNA FISH in intact insect appendages

Stefan Pentzold[1*], Veit Grabe[2], Andrei Ogonkov[1], Lydia Schmidt[1], Wilhelm Boland[1] and Antje Burse[1]

Max Planck Institute for Chemical Ecology, [1]Department of Bioorganic Chemistry, [2]Department of Evolutionary Neuroethology, Hans-Knöll-Str. 8, D-07745 Jena, Germany
*corresponding author, email: spentzold@ice.mpg.de

Abstract

Optical imaging of gene expression by fluorescence *in situ* hybridisation (FISH) in insects is often impeded by their pigmented cuticle. Since most chemical bleaching agents are incompatible with FISH, we developed a RNA interference-based method for clearing cuticular pigmentation which enables using whole-mount body appendages for RNA FISH. Silencing *laccase2* or *tyrosine hydroxylase* in two leaf beetles species (*Chrysomela populi, Phaedon cochleariae*) cleared their pigmented cuticle and decreased light absorbance. Subsequently, intact appendages (palps, antennae, legs) from RNAi-cleared individuals were used to image expression and spatial distribution of antisense mRNA of two chemosensory genes (gustatory receptor, odorant-binding protein). Imaging did neither work for RNAi-controls due to retained pigmentation, nor for FISH-controls (sense mRNA). Several bleaching agents were incompatible with FISH, either due to degradation of RNA, lack of clearing efficacy or long incubation times. Overall, silencing pigmentation genes is a significant improvement over bleaching agents enabling FISH in intact appendages.

Key words: pigmentation, beetle cuticle, RNA interference, laccase2, tyrosine hydroxylase, whole-mount fluorescence *in situ* hybridisation

Summary statement:

Clearing cuticular pigmentation in beetles by gene silencing enables the use of intact appendages for fluorescence *in situ* hybridisation.

Introduction

Optical imaging in combination with *in situ* fluorescent labelling is a powerful method to elucidate spatiotemporal patterns of gene expression and to identify cellular circuits in biological systems (Lampasona and Czaplinski, 2016). For optimal image sharpness and resolution in fluorescence microscopy, samples should ideally be transparent. However, most tissues or appendages appear opaque and may be colored by pigments. These obstacles prevent imaging at high depth – or any optical penetration at all – into tissue due to light absorption and scattering, respectively (Richardson and Lichtman, 2015). Thus, sharp imaging, especially deep into a tissue volume such as from whole-mount preparations, becomes strongly limited. Alternatively, physical serial sectioning in ultra-thin slices may be performed; however, correcting single slices for alignment, geometric distortion and staining variation is time-demanding and can be error-prone (Zucker, 2006). Non-sectioning approaches such as optical sectioning by confocal laser scanning (cLSM) or light sheet microscopy, largely preserve the innate 3-dimensional structure of biological tissues and organs, but require transparent samples (Susaki and Ueda, 2016). Although a diverse set of novel tissue clearing techniques has been developed for some vertebrate species to achieve whole-organ or whole-body transparency enabling imaging of fluorescent labelled molecules deep into large tissue volume (Chung et al., 2013; Frétaud et al., 2017; Keller and Dodt, 2012; Li et al., 2017; Susaki et al., 2014; Susaki and Ueda, 2016; Tainaka et al., 2014; Yang et al., 2014), all current clearing methods come with specific limitations, e.g. they may affect structural and molecular integrity due to shrinkage or swelling of cells and tissue, quenching of fluorescence and/or altered antigenicity, among other issues (Li et al., 2017; Susaki and Ueda, 2016).

In many insect species, optical imaging is especially challenging, since pigmentation prevents fluorescence-based microscopy beneath the cuticle. Pigmentation and thus coloration can vary from colorless to yellowish or brownish to black depending on the amounts and types of melanin-like pigments incorporated (Barek et al., 2017). Such pigments absorb light which results in decreased laser intensity and low optical quality as one penetrates deeper into tissue (Smolla et al., 2014; Zucker, 2006). This bottleneck hampers deep imaging of intact tissue, appendages or whole bodies. Physical removal of the cuticle is less desirable due to inevitable destruction of surrounding tissue, especially in small specimen. Chemical clearing agents such as hydrogen peroxide (H_2O_2) bleach soft tissues such as brains, which allow fluorescent imaging of receptor neuron proteins by cLSM, but it results in tissue shrinkage

such as in ants (Smolla et al., 2014) or spherically expanded ruptures in hawkmoths (Stöckl and Heinze, 2015). Other bleaching protocols for whole insects with brownish bodies require at least three weeks of incubation (Kliot and Ghanim, 2016; Koga et al., 2009). Since many insect species such as beetles often possess a particular thick, hard and pigmented cuticle, here we present a novel methodological strategy that combines both specific and effective clearing of cuticular pigmentation as well as preservation of molecular and cellular integrity. This approach allows optical imaging of fluorescence-labelled polynucleotides in intact appendages or other whole-mount organs.

Materials and methods

Specimen, RNA extraction and cDNA synthesis

Poplar leaf beetles (*Chrysomela populi*, Linnaeus) were collected close to Dornburg (+51°00'52", +11°38'17") in Thuringia, Germany, where beetles were feeding on *Populus maximowiczii* x *Populus nigra* and reared in a climate chamber provided with fresh *P. nigra* under 16:8 h L:D cycles at 20°C. Mustard leaf beetles (*Phaedon cochleariae*, Fabricius) were lab-reared on *Brassica oleracea*. Both beetle species (Insecta: Coleoptera) belong to the tribe Chrysomelini within the family Chrysomelidae. After homogenizing adult beetles using mortar and pestle in liquid nitrogen RNA was purified using RNAqueous™ Total RNA Isolation Kit (Thermo Fisher Scientific Baltics UAB, Vilnius, Lithuania) including DNase treatment following the manufacturer's instruction. RNA concentration was measured on a NanoDrop™ One (Thermo Fisher Scientific, Madison, Wisconsin, U.S.). Synthesis of cDNA was carried out using SuperScript™ III Reverse Transcriptase and oligo(dT)$_{20}$ (Invitrogen™, Carlsbad, California, U.S.) following manufacturer's protocol.

Identification of candidate genes and molecular cloning

Orthologues of *Lac2* and *TH* in *C. populi* and *P. cochleariae* were identified by performing a BLAST search against the respective transcriptome (Stock et al., 2013; Strauss et al., 2014) using nucleotide sequences of *Lac2* (GenBank accession number: AY884061.2) and *TH* (EF592178) from *Tribolium castaneum* as template (Arakane et al., 2005; Gorman and Arakane, 2010). As targets for RNA FISH, a gustatory receptor (*CpopGR1*) and an odorant-binding protein (*CpopOBP13*) were identified from the transcriptome of *C. populi* (Strauss et al., 2014) by BLAST search using the template sequences CbowGR1 (GenBank: KT381521)

and CbowOBP13 (KT381495) from the cabbage beetle *Colaphellus bowringi* (Li et al., 2015) (Chrysomelini, Chrysomelidae). The sequence of the house-keeping gene actin from *C. populi* was obtained from GenBank (JX122919.1). Gene specific primers were designed using Primer3 software (see Table S1); a T7 promoter sequence (5'-TAATACGACTCACTATAGGGAGA-3') was appended to forward and reverse primers of *Lac2* (*CpopLac2*, *PcoLac2*) and *TH* (*CpopTH*, *PcoTH*) to allow dsRNA synthesis for RNA interference. PCR amplification was carried out using a proof-reading DNA polymerase (Phusion High-Fidelity F530S, Thermo Fisher Scientific, Madison, Wisconsin, U.S.). Amplicons were analyzed via gel electrophoresis, purified using QIAquick PCR Purification (Qiagen, Hilden, Germany) and sequenced. After RACE-PCR to verify full-length sequence using SMARTer RACE cDNA Amplification Kit (Clontech Laboratories, Mountain View, CA), *CpopGR1*, *CpopOBP13* and *CpopActin* were PCR-amplified without modification, sequenced and ligated into pCR-BluntII-TOPO (Invitrogen™, Carlsbad, California, U.S.) posseesing opposing T7 and SP6 promoter sequences to allow *in vitro* synthesis from one template for generation of sense and antisense probes for RNA FISH (see below: Synthesis of labelled RNA FISH probes).

RNA interference

Synthesis of dsRNA

Synthesis of double-stranded RNA (dsRNA) was carried out using MEGAscript® RNAi Kit (Applied Biosystems International, Zug, Switzerland) according to the manufacturer's recommendations. In brief, PCR product with opposing T7 promoters flanking the target sequences (*Lac2*, *TH* from *C. populi* or *P. cochleariae*) was transcribed *in vitro* by incubating for 6 h at 37°C with T7-Polymerase, ATP, CTP, GTP and UTP including RNase inhibitor protein. Formation of dsRNA was induced by incubating the reaction mixture for 5 min at 75°C and then cooling to room temperature (RT). After nuclease digestion of single-stranded RNA and DNA, dsRNA was purified using filter cartridges and centrifugation. Finally, dsRNA was ethanol precipitated, resuspended in 0.9% physiological NaCl and adjusted to approximately 1 µg/µl. The concentration and integrity of the dsRNA were determined by spectrometry (NanoDrop™ One) and gel electrophoresis. The following lengths of dsRNA were generated: *Cpop*ds*TH*: 535 bp, *Cpop*ds*Lac2*: 548 bp, *Pco*ds*Lac2*: 521 bp, *Pco*ds*TH*: 544 bp (all excluding 23bp T7-promoter sequence, see Table S1). DsRNA of *Gfp* (719 bp) was used as control.

Microinjection

Microinjections were performed using pulled borosilicate glass capillaries and Nanoliter 2000 injector (both World precision instruments, Sarasota, Florida, U.S.). Injection was parasagittally between the pro- and mesothorax of either last larval instars or 3-day old pupae of *C. populi* and *P. cochleariae*. Insects were anesthetized on ice before and during injection. Each specimen was injected 20, 80 or 140 ng, respectively of total dsRNA. Twelve biological replicates were run per dsRNA treatment (*Lac2*, *TH*; *Gfp* as control) and amount, i.e. a total of 108 biological replicates. Additionally, 80 ng of each dsLac2 and dsTH were injected combined in young pupae. Five to ten days after eclosure and rearing adult beetles on *P. nigra*, chemosensory appendages such as legs, antennae and palps were dissected for use in RNA FISH (see below). Additionally, efficacy of RNAi-mediated knockdown of *CpopLac2* and *CpopTH* was assessed using quantitative real-time PCR on cDNA derived from legs. Therefore, transcript abundance of *Lac2* or *TH* in ds*Gfp* control samples was set as baseline (100%) and compared to their expression in RNAi beetles. For statistical analysis, mean ct values of *Lac2* or *TH* from both groups (ds*Gfp* control *versus* RNAi) were compared for significant differences using Wilcoxon Rank-Sum test using SigmaPlot 12.0 (Systat Software, Erkrath, Germany). Five biological replicates were analyzed from both groups. For primers see Table S1.

Quantitative real time-PCR

Using qRT-PCR transcript abundance of (i) *Lac2* and *TH* was analyzed in *C. populi* in larvae, pupae and adults, and in adult legs, antennae and wings (three to four biological replicates), (ii) *CpopGR1* and *CpopOBP13* in adult tissues such as gut, wings, thorax (excluding head and legs), legs, antennae and head including palps (six biological replicates). Data were quantified relative to the mRNA levels of the reference genes eukaryotic elongation factor 1-alpha (*EF1a*) and initiation factor 4A (eIF4A) using the $2^{-\Delta\Delta Ct}$ method (Livak and Schmittgen, 2001) and multiplied by 1000. Data were acquired on a CFX-96 Touch™ Real-Time PCR Detection System (Bio-Rad Laboratories, Hercules, California, U.S.) using Brilliant III Ultra-Fast SYBR® Green QPCR Master Mix (Agilent Technologies, Cedar Creek, Texas, U.S.) and cDNA as template. Distilled water as template served as negative control. Two technical replicates were analyzed; those with a Ct difference of >0.5 were repeated. To exclude effects of RNAi (ds*Lac2*, ds*Gfp*) on the expression level of *CpopGR1* and *CpopOBP13* (as RNA FISH targets, see below), their expression was compared to ds*Lac2* or ds*Gfp*-injected individuals by qRT-PCR on cDNA derived from of legs (five biological replicates per group).

Statistical difference of the $^{\Delta Ct}$-values between the two groups was compared using t-test (SigmaPlot 12.0, Systat Software, Erkrath, Germany). Standard curves in five different 10-fold dilutions were used to calculate amplification efficiency. For each primer pair sigmoidal amplification curves were obtained with single melt curve peaks. No signals were detected for the negative controls. For primers used see Table S1.

Absorbance measurement

Three legs from *C. populi* beetles that were silenced in *Lac2*, *TH* or control individuals were ground in 6M HCl and centrifuged to pellet cell and tissue debris. Supernatant was used to measure absorbance from 400 to 800 nm per milligram ground tissue on a UV/VIS spectrophotometer (Jasco V-550, Jasco, Pfungstadt, Germany).

Whole-mount double RNA FISH (fluorescence *in situ* hybridisation)

Synthesis of labelled RNA FISH probes

Plasmids containing target sequences (*CpopGR1*, *CpopOBP13*, *CpopActin*) flanked by opposing T7 and SP6 promoter sequences were linearized using NotI or BamHI. Subsequent *in vitro* transcription of fluorescence-labelled antisense or sense RNA was carried out using SP6 or T7 DNA-dependent RNA polymerases (Thermo Fisher Scientific, Madison, Wisconsin, U.S.) in the presence of biotin (*GR1*, *OBP13*) or digoxigenin (DIG; *actin*) following the according RNA Labelling mix (Roche, Mannheim, Germany). After incubation for 3 h at 37°C, RNA was precipitated using ethanol, dissolved in RNase-free water and diluted in hybridisation buffer: 50% deionized formamide, 2× saline sodium citrate buffer, 0.2 mg/mL UltraPure™ Herring Sperm DNA (Thermo Fisher Scientific, Madison, Wisconsin, U.S.), 200 µg/ml yeast tRNA (Roche, Mannheim, Germany), and 10% dextran sulfate (Calbiochem, Darmstadt, Germany) in double-distilled water. The following lengths were generated: *CpopGR1*: 390 nt and *CpopOBP13*: 513 nt (both biotin-labelled) and *CpopActin* (DIG-labelled) about 450 nt from original 1131 nt after incubation in hydrolysis buffer (80 mM $NaHCO_3$ and 120 mM Na_2CO_3) at 60°C for 14,5 min, formula see (Zimmerman et al., 2013).

Fixation and FISH procedure

Intact and whole-mount palps (labial, maxillary), antennae and legs were freshly dissected from ice-chilled adult *C. populi* beetles that were injected beforehand with either ds*Lac2*, ds*TH* or ds*Gfp* as control. Three independent biological replicates from each appendage and

injected dsRNA were used for FISH. To improve penetration of labelled FISH probes, antennae and legs were cross-sectioned into a distal and proximal part (at the 5th flagellomere or between tibia and femur, respectively). Samples were fixed in 4% paraformaldehyde in 1M $NaHCO_3$ at 4°C for 24 h. Organs were washed in 1x phosphate-buffered saline (PBS, pH 7,1) containing 0,03% Triton™ X-100 (Sigma-Aldrich, Darmstadt, Germany) for 1 min at RT and incubated in 0.2M HCl containing 0,03% Triton™ X-100 for 10 min. After washing in 1xPBS with 1% Triton™ X-100 for 1 min at RT, prehybridization was carried out by incubating samples in hybridisation buffer for 4 h at 4°C and for additional 6 h at 55°C. Hybridisation of labelled RNA probes to endogenous transcripts was performed at 55°C for 3 days. The following combinations were used: antisense or sense mRNA of *GR1* or *OBP13* in combination with antisense of actin. After washing in 0,1x saline sodium citrate buffer with 0,03% Triton™ X-100 four times at 60°C by horizontal shaking at 350 rpm, samples were blocked in 1%-blocking solution (Roche, Mannheim, Germany) diluted in tromethamin-buffered saline (TBS, pH 7,5) and 0,03% Triton™ X-100 for 6h at 4°C. Detection of DIG-labelled probes was achieved by using an anti-DIG-conjugated alkaline phosphatase (1:500) that dephosphorylates HNPP added to the sample into HNP that precipitates to RNA in the presence of Fast Red TR (HNPP Fluorescent Detection Set, Roche, Mannheim, Germany). Detection of biotin-labelled probes was achieved using streptavidin-coupled horse radish peroxidase (dilution 1:100) and tyramide signal amplification TSA fluorescein detection kit (Perkin Elmer, Waltham, Massachusetts, U.S.). In both cases, antibody incubation was carried out for 3 days at 4°C followed by substrate incubation for 6 h. Intermediate washing steps were carried out three times for 10 min in TBS with 0,05% Tween-20 (Sigma-Aldrich, Darmstadt, Germany). Counterstaining of cellular dsDNA was done using 4′,6-diamidino-2-phenylindole (DAPI) nucleic acid stain (Molecular Probes, Eugene, Oregon, U.S.) in 30 mM PBS and incubated for 30 min at RT in dark followed by three times washing in PBS. Finally, samples were transferred onto microscope slides covered in Vectashield® antifade mounting medium (Vector Laboratories, Burlingame, California, U.S.).

Microscopy and image processing

Fluorescent images were acquired with a ZEISS LSM 880 Confocal Laser Scanning Microscope using a 20x/0.8 Plan-Apochromat or 40x/1.2 C-Apochromat W (all Zeiss, Jena, Germany), respectively. Excitation of the fluorophores was conducted through a 405 nm laser diode, a 488 nm Argon laser and a 543 nm Helium-Neon laser (Zeiss, Jena, Germany). The systems spectral Quasar detector was setup to detect the fluorophores at 415-490 nm for

DAPI, 490-561 nm for biotin-labelled and 551-735 nm for DIG-labelled probes. The pinhole was adjusted to 1 airy unit for the crucial channel of the *in situ* probe. Reflected light brightfield images from whole beetles or appendages were obtained on an AXIO Zoom V.16 (Zeiss, Jena, Germany). Images were processed using the following imaging software: ZEN (Zeiss, Jena, Germany), Helicon Focus (HeliconSoft, Kharkiv, Ukraine), Fiji (Schindelin et al., 2012) and Photoshop® CS (Adobe Systems, San Jose, California, U.S.).

Chemical bleaching

Freshly dissected and fixed antennae and legs from *C. populi* were incubated in H_2O_2 (Sigma-Aldrich, Darmstadt, Germany) at different concentrations (aqueous 35%, 10%, or alcoholic 6%) versus water or ethanol controls at RT. In addition, whole beetles were incubated in 35% H_2O_2 for 5 days at RT. For incubation in methyl salicylate freshly dissected heads of *C. populi* were dehydrated in an ethanol series, transferred in glass vials containing 1:1 ethanol:methyl salicylate for incubation for 1 h and finally substituted by 100% methyl salicylate (Sigma-Aldrich, Darmstadt, Germany) for incubation for one week at RT during shaking (350 rpm). After dehydrating further samples in a methanol series, they were incubated in a 1:2 mixture of BABB (Benzyl alcohol/benzyl benzoate from Sigma-Aldrich, Darmstadt, Germany) and incubated for three weeks. Two independent biological replicates were analyzed for each combination.

RNA degradation

Degradation of cellular RNA was analyzed from antennae and legs (incubated for 3 days in 35% H_2O_2 or 6% alcoholic H_2O_2 in comparison to control incubations (water or ethanol) via qRT-PCR after RNA extraction and cDNA synthesis from three biological replicates (5-10 antennae or legs mixed) as described above. Therefore, mean $^{\Delta\Delta Ct}$-values of two reference genes (*EF1a* and *IF4a*) were compared between the two test and control treatments taking the latter values as baseline (100%) of mRNA abundance.

Data availability

The data that support the findings of this study are available from the corresponding author upon reasonable request. Sequences generated in this study are deposited in GenBank (www.ncbi.nlm.nih.gov/genbank) under the following accession numbers: *CpopLac2*: MH253687; *PcoLac2*: MH253688; *CpopTH*: MH253689; *PcoTH*: MH253690; *CpopGR1*: MH253691; *CpopOBP13*: MH253692.

Results and Discussion

We took advantage of the proven functional importance of the enzymes tyrosine hydroxylase (TH) and laccase2 (Lac2, a phenoloxidase) in the beetle's cuticular pigmentation pathway catalyzing the first and following enzymatic steps (Arakane et al., 2005; Noh et al., 2016) (Fig. 1A). As validated by qRT-PCR, *lac2* and *TH* were most expressed in the adult stage of the poplar leaf beetle (*C. populi*), especially in chemosensory appendages such as legs and antennae, which corresponds to the highest degree of pigmentation compared to other developmental stages and tissues, respectively (Fig. S1A). Silencing *TH* and *Lac2* by RNA interference (RNAi) resulted in significant clearing of cuticular pigmentation in comparison to RNAi-controls (ds*Gfp*) in adult *C. populi* as well as the mustard leaf beetle *P. cochleariae* (Fig. 1B). Injecting 140 ng dsRNA of *Lac2* or *TH* per individual was more efficient in clearing cuticular pigmentation than injecting only 80 ng dsRNA. Injection of ds*Lac2* or ds*TH* in young pupae reduced pigmentation already in late pupae, but not in controls (Fig. S2). Hatching rate was similar among ds*Lac2* (68,5%, N=46), ds*TH* (77,8%, N=22) and ds*Gfp*-control (65,8%, N=51) injected individuals. RNAi adults survived at least 8 days without any apparent adverse effects. Other studies using dipteran species reported pleiotropic effects of silencing *lac2* or *TH* such as impaired resistance (Du et al., 2017) or reduced immunity (Chen et al., 2018) after pathogenic infection. Importantly, in *C. populi* and *P. cochleariae* RNAi-based clearing of cuticular pigmentation was induced in chemosensory appendages such as antennae, legs and palps (Fig. 1B,C). Transcript levels were silenced significantly, i.e. by 94,5% and 98,2% for *CpopLac2* and *CpopTH* respectively in comparison to RNAi-controls, as validated by qRT-PCR (P=0.008, P=0.016; Fig. 1D).

To quantify clearing of cuticular pigmentation the visible spectrum of the supernatant of acid-macerated legs was measured by UV–Vis spectroscopy. The higher absorbance in the 400–475 nm region in RNAi-control samples, which is characteristic of brownish-colored products from insect cuticles (Barek et al., 2017), was missing in less pigmented *lac2*- and *TH*-RNAi samples (Fig. 1E) showing a mean reduction in light absorbance of 78,0 and 91,4%, respectively. Therefore, we tested whether RNAi-cleared specimens are suitable for whole-mount RNA FISH and optical imaging by cLSM without chemical bleaching that would likely degrade mRNA.

As RNA FISH targets, two distinct chemosensory gene families were chosen: a gustatory receptor (*CpopGR1*) and an odorant-binding protein (*CpopOBP13*). Both genes were most expressed in body appendages such the head (including palps), legs and antennae (Fig. S1B). Similar to other gene expression studies in beetles (Dippel et al., 2016; Dippel et al., 2014; Li et al., 2015), *CpopGR1* had relative low overall expression levels, even in chemosensory organs (~10% of reference genes), whereas OBPs such as *CpopOBP13* are generally higher expressed as shown for the chemosensory appendages of *C. populi* (up to 15 times higher than reference genes). The RNAi treatment did not affect RNA FISH target sequences, i.e. the expression levels of *GR1* and *OBP13* did not differ between RNAi individuals (ds*Lac2* and ds*TH*) compared to RNAi-controls (P=0,39 for *CpopGR1*; P=0,73 for *CpopOBP13*, t-test). For RNA FISH, whole-mount chemosensory appendages (palps, antennae and legs) from RNAi-*Lac2* and RNAi-*TH* cleared beetles were incubated with biotin-labelled antisense mRNA (or sense mRNA as control) targeting either *CpopGR1* or *CpopOBP13* and combined with digoxigenin-labelled *CpopActin* as housekeeping gene. Importantly, gene expression of *CpopGR1* and *CpopOBP13* in intact appendages was successfully imaged via cLSM in those individuals that were silenced in *Lac2* or *TH* (Fig. 2A, Fig. S3A,B). For example, cells expressing *CpopGR1* were mainly proximal in the palp (Fig. 2A, i) and overall less abundant than those expressing *CpopOBP13* showing a broader distribution (Fig. 2A, ii). This is similar to the expression measured via qRT-PCR indicating relatively low or high expression for *CpopGR1* or *CpopOBP13*, respectively (Fig. S1B). Furthermore, in the antennae, *CpopOBP13* was expressed in the proximal and more distal parts (Fig. S3A), whereas in the tibia *CpopOBP13* was mainly expressed in proximal cells (Fig. S3B). Cuticular autofluorescence in RNAi-cleared organs remains to some extant after optical sectioning by cLSM (e.g. Fig. 2A i, ii), which is most likely caused by chitin (Rabasović et al., 2015). In another study, H_2O_2-based quenching of autofluorescence was used to image microbial endosymbionts living in inner insect tissues such as the gut (Koga et al., 2009); in general, many tissue clearing methods do not necessarily remove background autofluorescence (Richardson and Lichtman, 2015). In contrast to RNAi-cleared specimens, optical imaging of *CpopGR1* and *CpopOBP13* was not possible in RNAi-controls (ds*Gfp*) due to retained pigmentation that prevented optical penetration (Fig. 2A, iii). As further controls, using sense mRNA for FISH did not result in specific fluorescence for *GR1* or *OBP13* in any of the RNAi-treated beetles (ds*Lac2*, ds*TH* or ds*Gfp*-controls) (Figs 2A, S3C). Nuclear DNA staining via fluorescent DAPI confirms cell integrity in RNAi-cleared tarsi of *C. populi* and *P. cochleariae* (Fig. 2B).

To corroborate that RNAi-based clearing of cuticular pigmentation is the means of choice for using whole-mount organs in RNA FISH, we show that several bleaching chemicals are not feasible FISH, either due to significant degradation of polynucleotides, lack of clearing efficacy or long incubation times. We first tested H_2O_2 of which hydroxyl radicals and OOH-groups are known to destroy the cuticle-pigment melanin (Korytowski and Sarna, 1990). Whereas incubation of dissected body appendages in 35% H_2O_2 for 3 days reduced cuticular pigmentation in legs (Fig. 2C), it degraded 99,2% of the total RNA in comparison to water-incubated controls (Fig. 2D); similarly, antennae were chemically bleached resulting in degradation of 91,6% total RNA (Fig. 2C,D). Incubation of antennae and legs for 3 days in water (Fig. 2C) or 10% H_2O_2 did not reduce cuticular pigmentation, but degraded RNA (Fig. 2D). When incubating in alcoholic 6% H_2O_2, it took at least three weeks until bleaching of intact or bipartite antennae and legs (Fig. S4A). This is similarly long to bleaching brown-colored, but relatively small insects such as lice, bat flies or aphids (Koga et al., 2009). However, almost two third of total RNA (63,7%) was degraded despite prior to tissue fixation. When whole beetles were incubated in 35% H_2O_2 for five days, cuticular decoloration was evident, but partly incomplete, especially on the legs and wings that were also damaged (Fig. S4B). Consequently, cell integrity in legs and antennae was not retained in H_2O_2-bleached samples as further indicated by unsuccessful DAPI staining (Fig. 2E). The cell-damaging characteristics of H_2O_2 resulting in degradation of total RNA and decreased fluorescence emission from green fluorescent proteins (Alnuami et al., 2008), makes this bleaching method unsuitable for (RNA) FISH. This is especially important when targeting lowly expressed genes such as most insect GRs (Dippel et al., 2016). Other clearing agents such as methyl salicylate (Zucker, 2006) did clear soft tissues such as the brain of *C. populi*, but retained cuticular pigmentation (Fig. S5A). Similarly, a mixture of benzyl alcohol/benzyl benzoate did not clear cuticular pigmentation in antennae or legs (Fig. S5B).

Overall, RNAi-based clearing of cuticular pigmentation is a significant improvement compared to chemical bleaching agents, since it preserves molecular and cellular integrity and enables FISH deep into tissue of intact whole-mount samples. This makes serial sectioning of organs redundant. We expect that our method also works with other, non-chemosensory genes as FISH targets regardless of whether they encode soluble proteins or membrane receptors, or whether they are lowly or highly expressed. Moreover, since RNAi-based suppression of Lac2 or TH decreases cuticular pigmentation in different coleopteran (Gorman and Arakane, 2010; Niu et al., 2008; Powell et al., 2017) and several other non-coleopteran insect species (Chen et al., 2018; Elias-Neto et al., 2010; Futahashi et al., 2011; Liu et al., 2010; Okude et

al., 2017), our method could be adapted to many other hexapod species enabling investigations beyond transparent embryos or ovaries. Imaging beneath the RNAi-cleared cuticle may further benefit from light sheet microscopy that minimizes fluorophore bleaching and phototoxic effects. Finally, RNAi-based cuticle clearing complements existing toolkits such as by enabling *in vivo* calcium imaging, in contrast to chemical bleaching which does not maintain most life functions

Acknowledgements: We are grateful to Vera L. Hopfenmüller for running replicates of FISH and to Tobias Becker for setting up the absorbance measurement.

Competing interests: The authors declare no competing interests.

Author contributions: S.P., W.B. and A.B. conceived and designed the study. S.P. performed RNA extractions, cDNA synthesis, identification of candidate genes, molecular cloning, qRT-PCR, FISH probe synthesis, fixation and RNA degradation assay. S.P. and A.O. performed chemical bleachings. V.G. carried out microscopic analyses by cLSM, processed images and constructed illustrations. A.O. analyzed RNAi efficacy, performed dsRNA microinjection and FISH procedure. A.O. and A.B. analyzed survival of RNAi beetles. L.S. synthesized dsRNA, did microinjections and prepared buffer solutions. S.P., A.O., V.G. and A.B. analyzed the data. S.P. wrote the manuscript, all authors revised it.

Funding: S.P. received project funding from the European Union's Horizon 2020 research and innovation programme under the Marie Skłodowska-Curie grant agreement No 705151. Further financial support from the Max Planck Society is acknowledged.

References:

Alnuami, A. A., Zeedi, B., Qadri, S. M. and Ashraf, S. S. (2008). Oxyradical-induced GFP damage and loss of fluorescence. *Int. J. Biol. Macromol.* **43**, 182-186.

Arakane, Y., Muthukrishnan, S., Beeman, R. W., Kanost, M. R. and Kramer, K. J. (2005). Laccase 2 is the phenoloxidase gene required for beetle cuticle tanning. *Proc. Natl. Acad. Sci. U. S. A.* **102**, 11337-11342.

Barek, H., Evans, J. and Sugumaran, M. (2017). Unraveling complex molecular transformations of N-β-alanyldopamine that accounts for brown coloration of insect cuticle. *Rapid Commun. Mass Spectrom.* **31**, 1363–1373.

Barek, H., Sugumaran, M., Ito, S. and Wakamatsu, K. (2018). Insect cuticular melanins are distinctly different from those of mammalian epidermal melanins. *Pigment Cell Melanoma Res.* **31**, 384-392.

Chen, E. H., Hou, Q. L., Wei, D. D., Dou, W., Liu, Z., Yang, P. J., Smagghe, G. and Wang, J. J. (2018). Tyrosine hydroxylase coordinates larval–pupal tanning and immunity in oriental fruit fly (*Bactrocera dorsalis*). *Pest Manage. Sci.* **74**, 569-578.

Chung, K., Wallace, J., Kim, S.-Y., Kalyanasundaram, S., Andalman, A. S., Davidson, T. J., Mirzabekov, J. J., Zalocusky, K. A., Mattis, J. and Denisin, A. K. (2013). Structural and molecular interrogation of intact biological systems. *Nature* **497**, 332-337.

Dippel, S., Kollmann, M., Oberhofer, G., Montino, A., Knoll, C., Krala, M., Rexer, K.-H., Frank, S., Kumpf, R. and Schachtner, J. (2016). Morphological and transcriptomic analysis of a beetle chemosensory system reveals a gnathal olfactory center. *BMC Biol.* **14**, 90.

Dippel, S., Oberhofer, G., Kahnt, J., Gerischer, L., Opitz, L., Schachtner, J., Stanke, M., Schutz, S., Wimmer, E. A. and Angeli, S. (2014). Tissue-specific transcriptomics, chromosomal localization, and phylogeny of chemosensory and odorant binding proteins from the red flour beetle *Tribolium castaneum* reveal subgroup specificities for olfaction or more general functions. *BMC Genomics* **15**, 1141.

Du, M.-H., Yan, Z.-W., Hao, Y.-J., Yan, Z.-T., Si, F.-L., Chen, B. and Qiao, L. (2017). Suppression of Laccase 2 severely impairs cuticle tanning and pathogen resistance during the pupal metamorphosis of *Anopheles sinensis* (Diptera: Culicidae). *Parasit. Vectors* **10**, 171.

Elias-Neto, M., Soares, M. P., Simões, Z. L., Hartfelder, K. and Bitondi, M. M. (2010). Developmental characterization, function and regulation of a Laccase2 encoding gene in the honey bee, *Apis mellifera* (Hymenoptera, Apinae). *Insect Biochem. Mol. Biol.* **40**, 241-251.

Frétaud, M., Rivière, L., De Job, É., Gay, S., Lareyre, J.-J., Joly, J.-S., Affaticati, P. and Thermes, V. (2017). High-resolution 3D imaging of whole organ after clearing: taking a new look at the zebrafish testis. *Sci. Rep.* **7**, 43012.

Futahashi, R., Tanaka, K., Matsuura, Y., Tanahashi, M., Kikuchi, Y. and Fukatsu, T. (2011). Laccase2 is required for cuticular pigmentation in stinkbugs. *Insect Biochem. Mol. Biol.* **41**, 191-196.

Gorman, M. J. and Arakane, Y. (2010). Tyrosine hydroxylase is required for cuticle sclerotization and pigmentation in *Tribolium castaneum*. *Insect Biochem. Mol. Biol.* **40**, 267-273.

Keller, P. J. and Dodt, H.-U. (2012). Light sheet microscopy of living or cleared specimens. *Curr. Opin. Neurobiol.* **22**, 138-143.

Kliot, A. and Ghanim, M. (2016). Fluorescent in situ hybridization for the localization of viruses, bacteria and other microorganisms in insect and plant tissues. *Methods* **98**, 74-81.

Koga, R., Tsuchida, T. and Fukatsu, T. (2009). Quenching autofluorescence of insect tissues for in situ detection of endosymbionts. *Appl. Entomol. Zool.* **44**, 281-291.

Korytowski, W. and Sarna, T. (1990). Bleaching of melanin pigments. Role of copper ions and hydrogen peroxide in autooxidation and photooxidation of synthetic dopa-melanin. *J. Biol. Chem.* **265**, 12410-12416.

Lampasona, A. A. and Czaplinski, K. (2016). RNA voyeurism: A coming of age story. *Methods* **98**, 10-17.

Li, W., Germain, R. N. and Gerner, M. Y. (2017). Multiplex, quantitative cellular analysis in large tissue volumes with clearing-enhanced 3D microscopy (Ce3D). *Proc. Natl. Acad. Sci. U. S. A.* **114**, E7321-E7330.

Li, X. M., Zhu, X. Y., Wang, Z. Q., Wang, Y., He, P., Chen, G., Sun, L., Deng, D. G. and Zhang, Y. N. (2015). Candidate chemosensory genes identified in *Colaphellus bowringi* by antennal transcriptome analysis. *BMC Genomics* **16**, 1028.

Liu, C., Yamamoto, K., Cheng, T.-C., Kadono-Okuda, K., Narukawa, J., Liu, S.-P., Han, Y., Futahashi, R., Kidokoro, K. and Noda, H. (2010). Repression of tyrosine hydroxylase is responsible for the sex-linked chocolate mutation of the silkworm, *Bombyx mori*. *Proc. Natl. Acad. Sci. U. S. A.* **107**, 12980-12985.

Livak, K. J. and Schmittgen, T. D. (2001). Analysis of relative gene expression data using real-time quantitative PCR and the $2^{-(DD\ CT)}$ method. *Methods* **25**, 402-408.

Niu, B. L., Shen, W. F., Liu, Y., Weng, H. B., He, L. H., Mu, J. J., Wu, Z. L., Jiang, P., Tao, Y. Z. and Meng, Z. Q. (2008). Cloning and RNAi-mediated functional characterization of MaLac2 of the pine sawyer, *Monochamus alternatus*. *Insect Mol. Biol.* **17**, 303-312.

Noh, M. Y., Muthukrishnan, S., Kramer, K. J. and Arakane, Y. (2016). Cuticle formation and pigmentation in beetles. *Curr. Opin. Insect Sci.* **17**, 1-9.

Okude, G., Futahashi, R., Kawahara-Miki, R., Yoshitake, K., Yajima, S. and Fukatsu, T. (2017). Electroporation-mediated RNA interference reveals a role of the multicopper oxidase 2 gene in dragonfly cuticular pigmentation. *Appl. Entomol. Zool.* **52**, 379-387.

Powell, M. E., Bradish, H. M., Gatehouse, J. A. and Fitches, E. C. (2017). Systemic RNAi in the small hive beetle *Aethina tumida* Murray (Coleoptera: Nitidulidae), a serious pest of the European honey bee *Apis mellifera*. *Pest Manage. Sci.* **73**, 53-63.

Rabasović, M. D., Pantelić, D. V., Jelenković, B. M., Ćurčić, S. B., Rabasović, M. S., Vrbica, M. D., Lazović, V. M., Ćurčić, B. P. and Krmpot, A. J. (2015). Nonlinear microscopy of chitin and chitinous structures: a case study of two cave-dwelling insects. *J. Biomed. Opt.* **20**, 016010.

Richardson, D. S. and Lichtman, J. W. (2015). Clarifying tissue clearing. *Cell* **162**, 246-257.

Schindelin, J., Arganda-Carreras, I., Frise, E., Kaynig, V., Longair, M., Pietzsch, T., Preibisch, S., Rueden, C., Saalfeld, S. and Schmid, B. (2012). Fiji: an open-source platform for biological-image analysis. *Nat. Methods* **9**, 676.

Smolla, M., Ruchty, M., Nagel, M. and Kleineidam, C. J. (2014). Clearing pigmented insect cuticle to investigate small insects' organs in situ using confocal laser-scanning microscopy (cLSM). *Arthropod Struct. Dev.* **43**, 175-181.

Stock, M., Gretscher, R. R., Groth, M., Eiserloh, S., Boland, W. and Burse, A. (2013). Putative sugar transporters of the mustard leaf beetle *Phaedon cochleariae*: their phylogeny and role for nutrient supply in larval defensive glands. *PLoS One* **8**, e84461.

Stöckl, A. L. and Heinze, S. (2015). A clearer view of the insect brain—combining bleaching with standard whole-mount immunocytochemistry allows confocal imaging of pigment-covered brain areas for 3D reconstruction. *Front. Neuroanat.* **9**, 121.

Strauss, A. S., Wang, D., Stock, M., Gretscher, R. R., Groth, M., Boland, W. and Burse, A. (2014). Tissue-specific transcript profiling for ABC transporters in the sequestering larvae of the phytophagous leaf beetle *Chrysomela populi*. *PLoS One* **9**, e98637.

Susaki, E. A., Tainaka, K., Perrin, D., Kishino, F., Tawara, T., Watanabe, T. M., Yokoyama, C., Onoe, H., Eguchi, M., Yamaguchi, S. et al. (2014). Whole-brain imaging with single-cell resolution using chemical cocktails and computational analysis. *Cell* **157**, 726-739.

Susaki, E. A. and Ueda, H. R. (2016). Whole-body and whole-organ clearing and imaging techniques with single-cell resolution: toward organism-level systems biology in mammals. *Cell Chem. Biol.* **23**, 137-157.

Tainaka, K., Kubota, S. I., Suyama, T. Q., Susaki, E. A., Perrin, D., Ukai-Tadenuma, M., Ukai, H. and Ueda, H. R. (2014). Whole-body imaging with single-cell resolution by tissue decolorization. *Cell* **159**, 911-24.

Yang, B., Treweek, J. B., Kulkarni, R. P., Deverman, B. E., Chen, C. K., Lubeck, E., Shah, S., Cai, L. and Gradinaru, V. (2014). Single-cell phenotyping within transparent intact tissue through whole-body clearing. *Cell* **158**, 945-958.

Zimmerman, S. G., Peters, N. C., Altaras, A. E. and Berg, C. A. (2013). Optimized RNA ISH, RNA FISH and protein-RNA double labeling (IF/FISH) in drosophila ovaries. *Nat. Protoc.* **8**, 2158.

Zucker, R. M. (2006). Whole insect and mammalian embryo imaging with confocal microscopy: morphology and apoptosis. *Cytometry A* **69**, 1143-52.

Figures

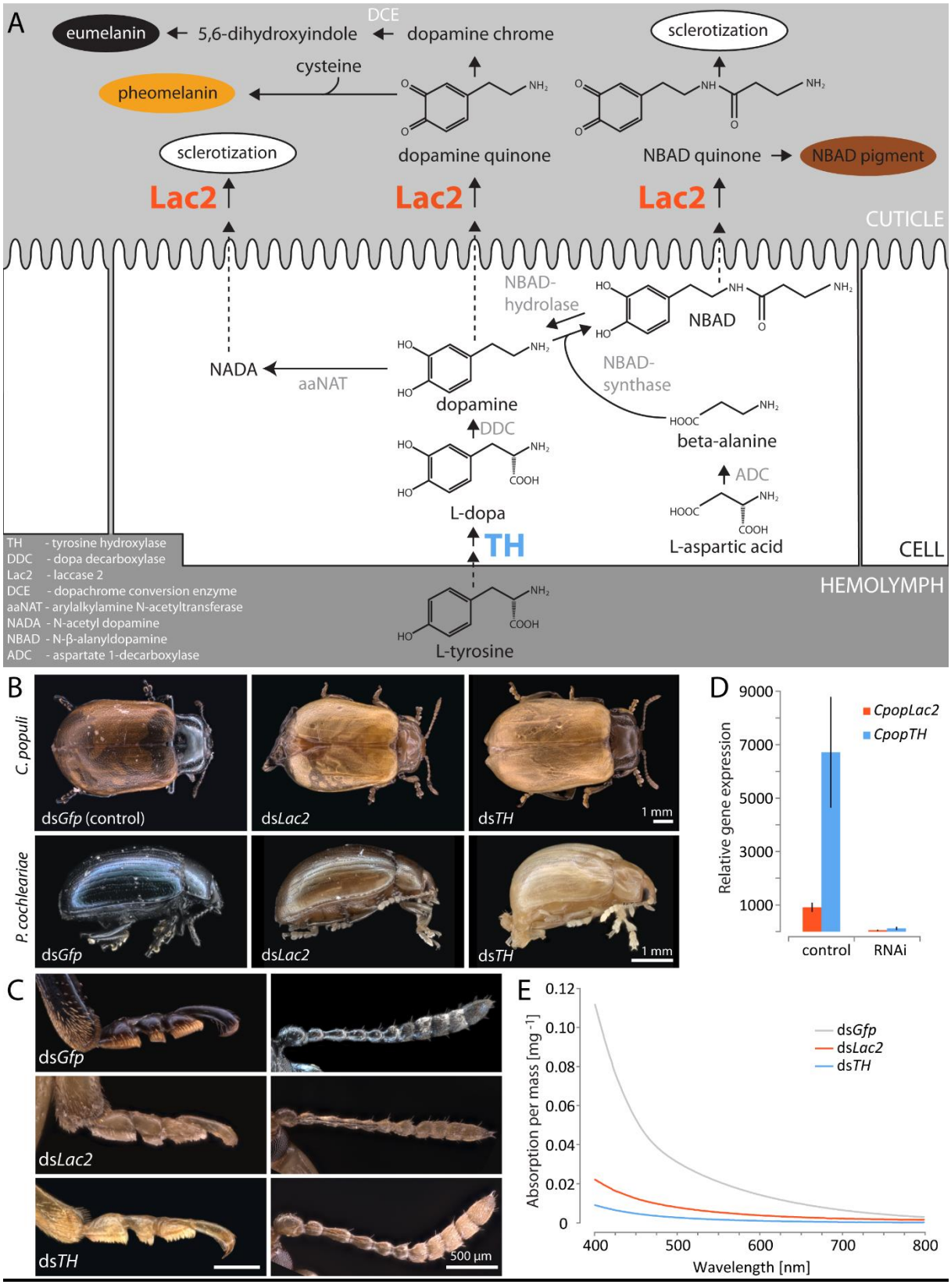

Figure 1. Silencing *TH* and *Lac2* genes by RNAi reduces cuticular pigmentation in adult leaf beetles. **A**. Tyrosine-derived cuticular pigmentation pathway in insects illustrating the involvement of tyrosine hydroxylase (TH, blue) and Laccase2 (Lac2, orange) enzymes with their respective substrates. The resulting pigments are colored as proposed by (Barek et al., 2018; Noh et al., 2016). **B:** Phenotypes of adult *C. populi* and *P. cochleariae* beetles silenced in *Lac2* and *TH* by RNAi (140 ng dsRNA per individual) are less pigmented and thus paler than RNAi-controls (ds*Gfp* injection). N=12 biol. replicates per gene and species. Injection of 80 ng ds*Lac2* or ds*TH* was less efficient for clearing pigmentation, while 20 ng were not efficient (not shown). **C:** Detail on chemosensory appendages such as tarsi (left) and antennae (right) of RNAi and control individuals indicating cleared pigmentation. **D**: Efficacy of RNAi-mediated silencing of *CpopLac2* and *CpopTH* in comparison to RNAi-controls (injection of ds*Gfp*) as analyzed by qRT-PCR. Differences in relative expression are statistically significant between the two treatments (*Lac2*: P=0,008; *TH*: P=0,016; Wilcoxon-Rank-Sum test) and refer to 94,5% and 98,2% respectively, transcript silencing in comparison to RNAi-controls. Bars represent mean±s.e.m; N=5 biol. replicates per treatment. **E:** Visible spectral changes measured by UV-Vis spectroscopy are associated with silencing *Lac2* or *TH* by RNAi in comparison to RNAi-controls (ds*Gfp*). Mean reduction in absorbance was 78% for ds*Lac2* and 91,4% for ds*TH*. Legs were macerated in acid and absorbance of the supernatant was measured from 400 – 800 nm.

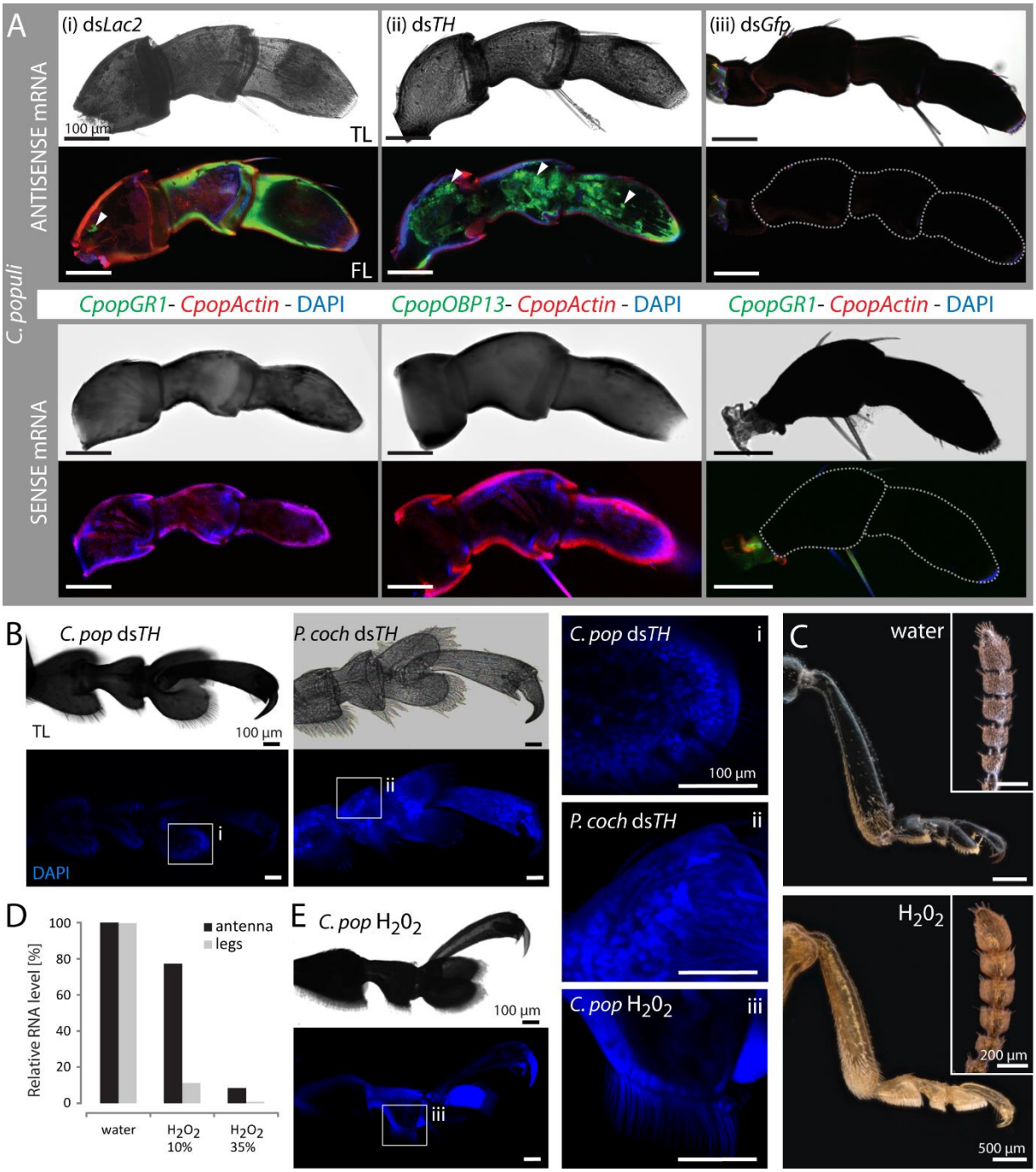

Figure 2. **Specific clearing of cuticular pigmentation by RNAi enables RNA FISH in whole-mount appendages of leaf beetles**. **A:** Maxillary palps from (i) *Lac2* or (ii) *TH*-silenced individuals with biotin-labelled mRNA of either a gustatory receptor (*CpopGR1*) or an odorant-binding protein (*CpopOBP13*) (both green) in combination with digoxigenin-labelled mRNA for *CpopActin* (red) as well as nuclear staining via DAPI (blue fluorescence). Due to remained pigmentation in RNAi-controls (ds*Gfp*, iii) FISH using the same mRNA probes was not possible. Whereas antisense mRNA binds to the target sequence (upper panels, arrowheads), sense mRNA of *GR1* or *OBP13* as control does not bind (lower panels). TL - transmitted light microscopy (light panels), FL – fluorescence image from confocal laser scanning microscopy (dark panels). **B:** Tarsi of *C. populi* and *P. cochleariae* cleared by silencing *TH* and stained with DAPI targeting nuclear dsDNA confirms cellular integrity of RNAi treatments (i, ii). **C:** Incubation of antennae and legs of *C. populi* in H_2O_2 (35%) for 3 days clears cuticular pigmentation in comparison to water-controls, but **D**: results in degradation of total RNA in both organs (bars represent mean of three biol. replicates per treatment). **E**: Tarsi incubated in H_2O_2 for 3 days could not be stained by DAPI indicating cellular damage by H_2O_2. Fluorescence is cuticular autofluorescence (iii). N=3 biol. replicates for each treatment.

Supplementary material

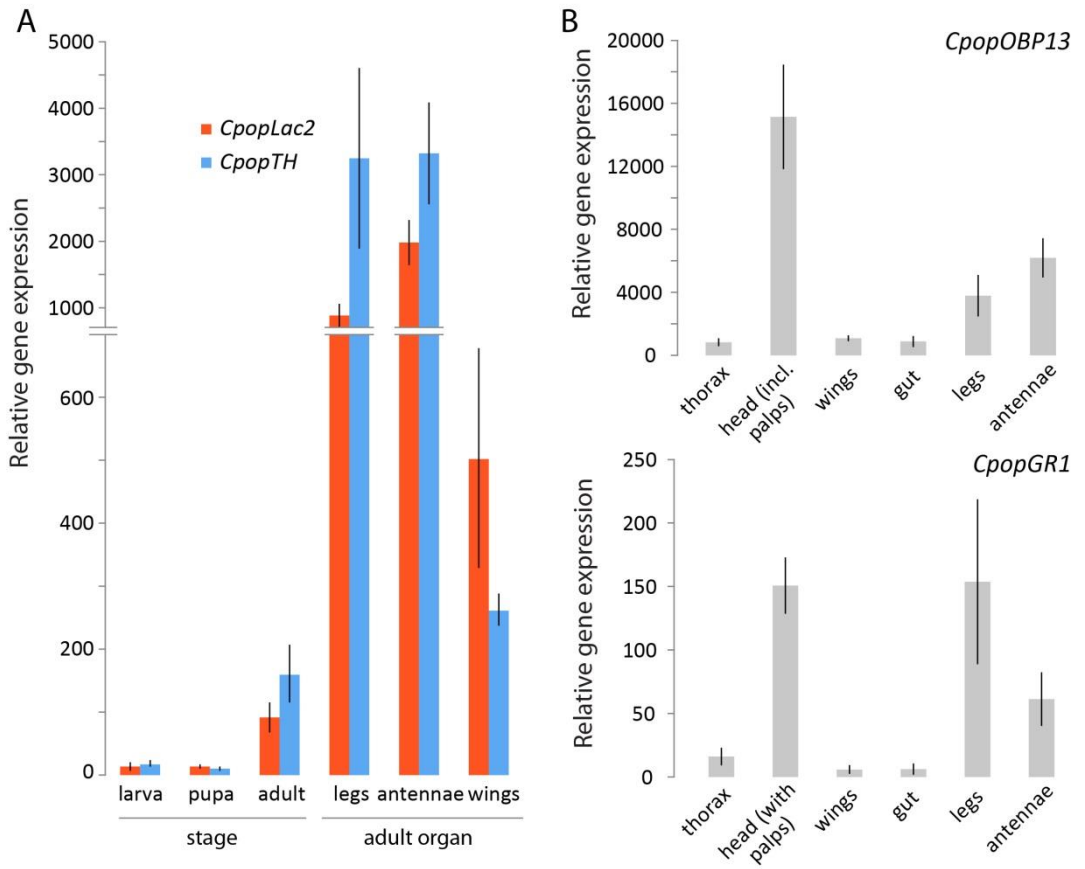

Supplementary Figure S1. **A:** Expression of *Laccase2* (*Lac2*) or *Tyrosine hydroxylase (TH)* as RNAi targets in untreated stages and adult tissues of *Chrysomela populi* as analyzed by qRT-PCR. N=4 biol. replicates, except larva, pupa and wings (N=3). **B:** Expression of the gustatory receptor *CpopGR1* and odorant-binding protein *CpopOBP13* as RNA FISH targets in untreated tissues of adult *C. populi* as analyzed by qRT-PCR. N=6 biol. replicates per tissue. Bars represent mean±s.e.m

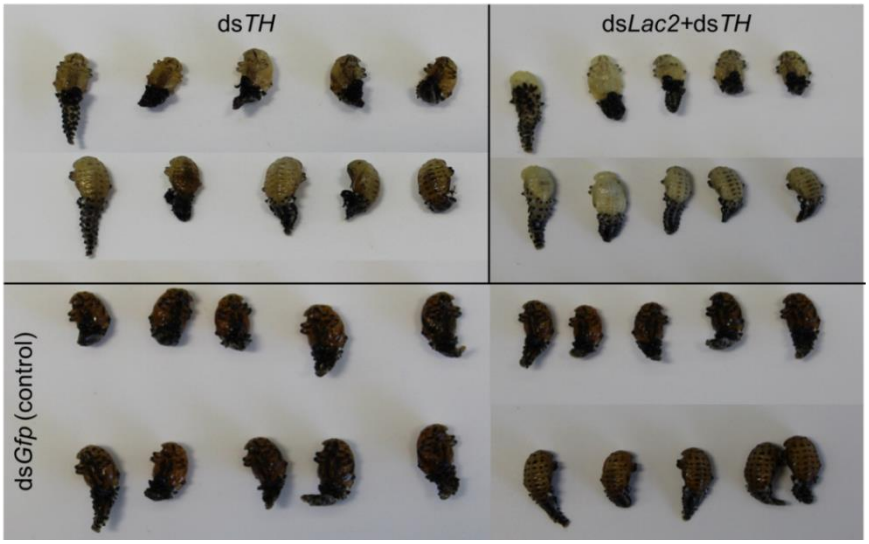

Supplementary Figure S2. Young *C. populi* pupae of the same age were injected dsRNA targeting *TH* or *Lac2 + TH* combined. RNAi-based clearing of cuticular pigmentation was evident in both cases already in late pupae in comparison to darker RNAi-controls (ds*Gfp* injection). N=12 biol. replicates for each treatment.

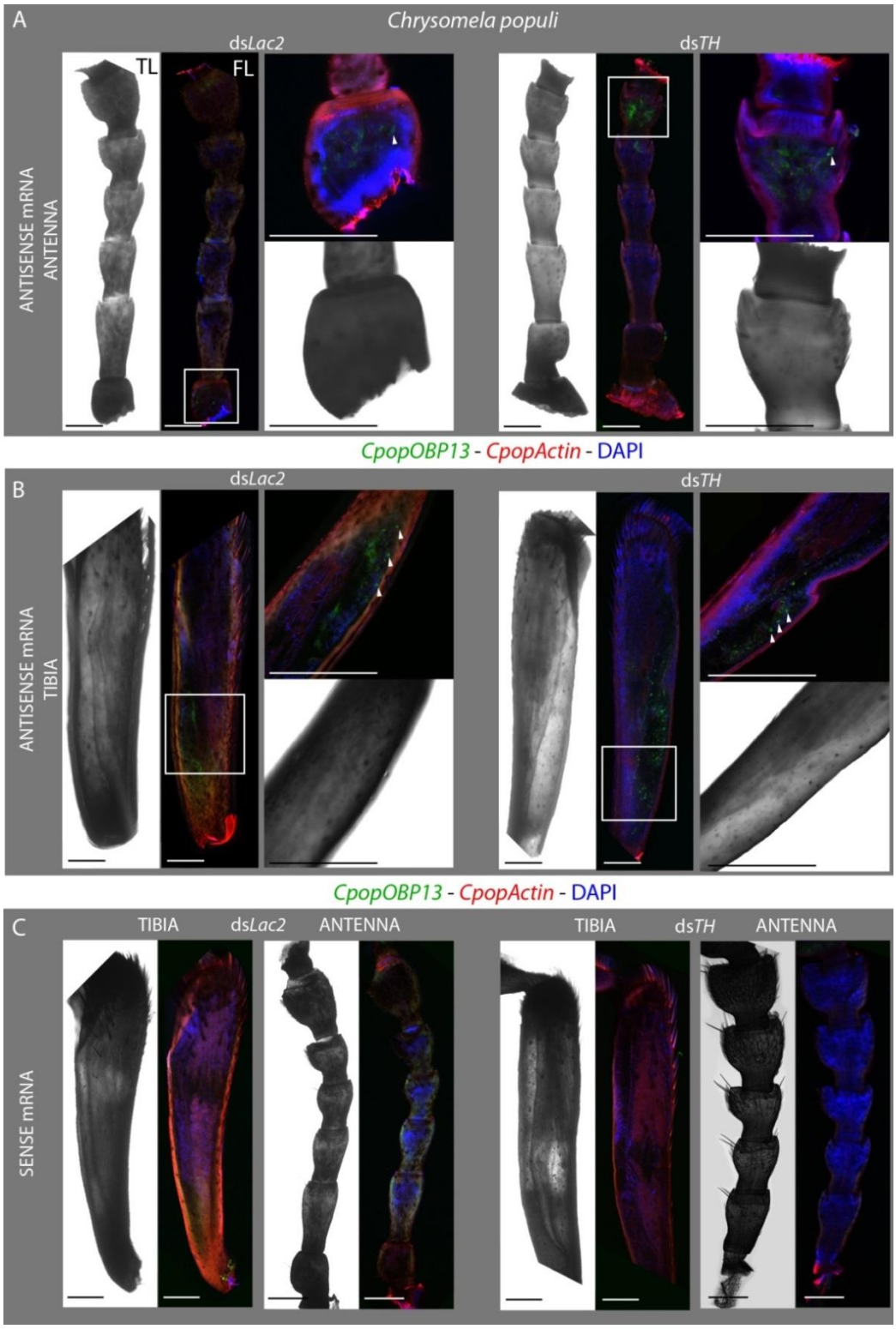

Supplementary Figure S3. Clearing of cuticular pigmentation by RNAi enables FISH in whole-mount appendages of *C. populi*. **A:** Antennae and **B:** tibiae from *Lac2* or *TH*-silenced individuals with biotin-labelled antisense mRNA of an odorant-binding protein (*CpopOBP13*) (green fluorescence) in combination with digoxigenin-labelled antisense mRNA for *CpopActin* (red) as well as DAPI staining nuclear dsDNA (blue). **C:** Using sense mRNA of *OBP13* as negative control in both RNAi-cleared appendages did not result in distinct green fluorescence, whereas positive controls (antisense *CpopActin*, DAPI) resulted in similar fluorescent signals as in A and B. Arrowheads indicate exemplary stained cells. Proximal parts of the organs are at the bottom, and distal part at the top of the image. TL - transmitted light microscopy (light panels), FL - fluorescence image from confocal laser scanning microscopy. N=3 biol. replicates for each treatment. Scale bar represents 200 µm.

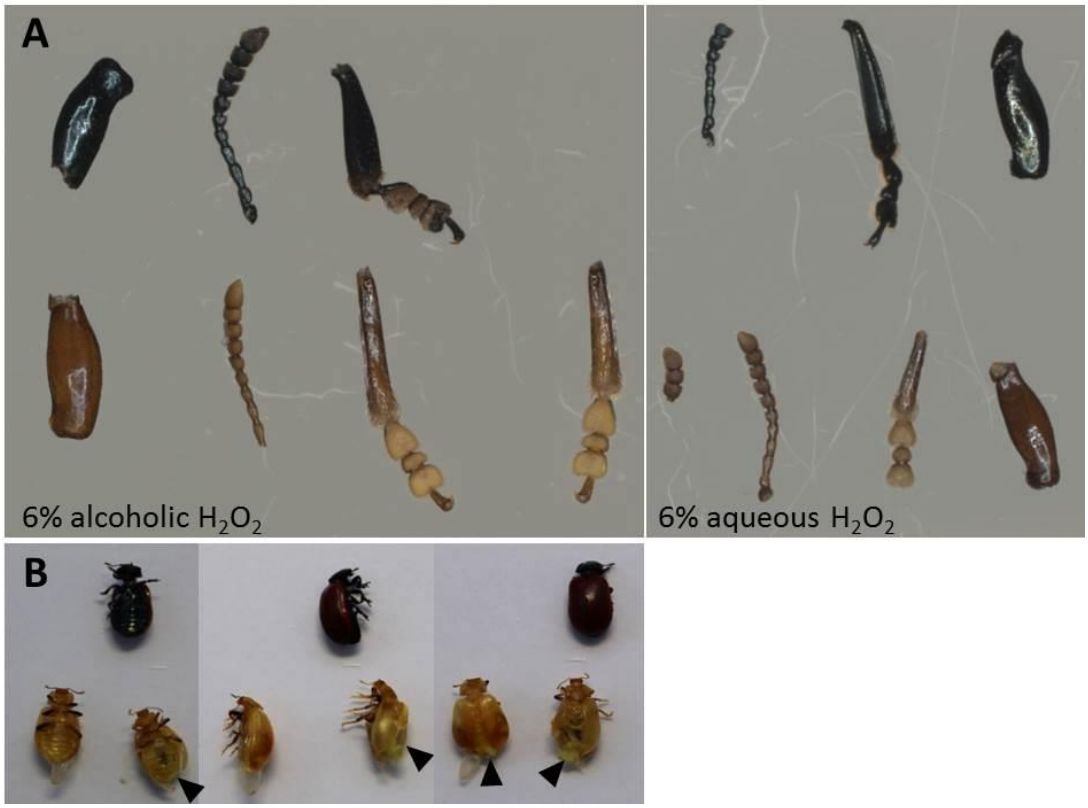

Supplementary Figure S4. **A:** Incubation of antennae and bipartite legs from *C. populi* in 6% alcoholic or aqueous H_2O_2 for three weeks clears pigmentation in comparison to control incubations (ethanol or water), but degrades RNA (see Fig. 1D). **B:** Incubation of whole beetles in 35% H_2O_2 (bottom row) for five days results in cuticular decoloration (in comparison to controls, top row), which is however partly incomplete, especially on the legs while in some cases organs such as wings were damaged (arrowheads). Two biological replicates per treatment were analyzed.

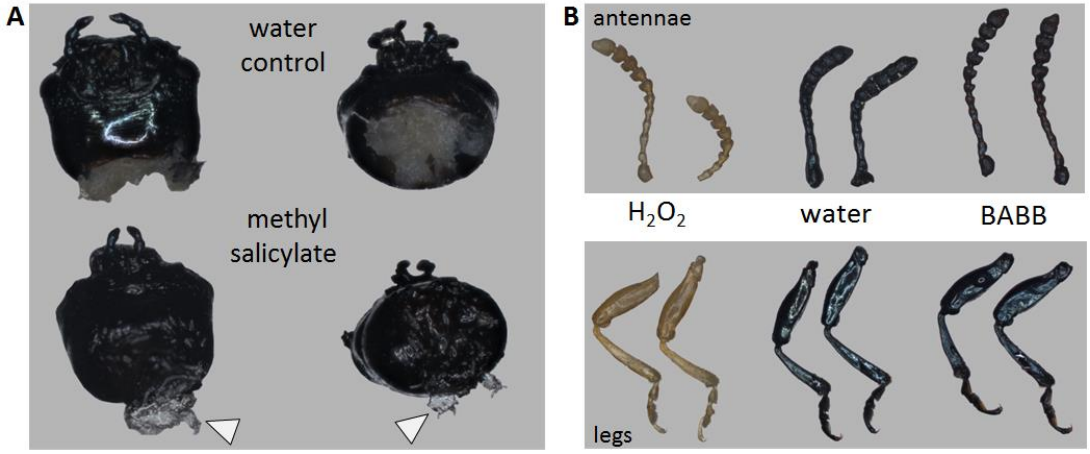

Supplementary Figure S5. Incubation of chemosensory appendages of *C. populi* in **A:** methyl salicylate for one week cleared soft tissue such as the brain (arrowheads), but not the cuticle; **B:** BAAB (1:2 benzyl alcohol/benzyl benzoate) for three weeks did not clear cuticular pigmentation of antennae or legs in contrast to incubation in 35% H_2O_2 as control. Two biological replicates per treatment were analyzed. All incubations were done after fixating and dehydrating samples.

Supplementary Table S1. **Primer sequences used for qRT-PCR, RNAi and RNA FISH**. Cpop – *C. populi*; Pco – *Phaedon cochleariae.* T7 promoter sequence in italics. eIF4A – eukaryotic initiation factor 4 alpha; EF1 – eukaryotic elongation factor 1; Lac2 – laccase2; TH – tyrosine hydroxylase; GR – gustatory receptor; OBP – odorant binding protein; fw – forward; rev – reverse.

Primer name	
qRT-PCR:	**5‘-3’- sequence**
CpopeIF4A_fw	TTTGTAATACCCGCCGCAAG
CpopeIF4A_rev	TCCATGCATCGCAGAAACAG
CpopEF1a_fw	TCATCGGTCACGTAGATTCTGG
CpopEF1a_rev	TTTCGATGGTACGCTTGTCG
CpopLac2q_fw	CTCGTTTTCTGGAGAGAGATAC
CpopLac2q_rev	CCAATCCTCTGAGTTGTATCC
CpopTHq_fw	CTAATGACTCCAGTGTAGAACC
CpopTHq_rev	GACGACTTCTTCTTCTGTGAG
CpopGR1q_fw	AGCTCCAGACAGTTCCTTTC
CpopGR1q_rev	AGATCTGGGTTGATGTCTTCGAG
CpopOBP13q_fw	GCCAAGACCAAGAAGGGAGAAT
CpopOBP13q_rev	GATTTTGCCTTGTGCGTCCATG
RNAi:	
CpopLac2_ rnai_fw	*TAATACGACTCACTATAGGG*AACGCTGGTACCCACTTCTG
CpopLac2_ rnai_rev	*TAATACGACTCACTATAGGG*GTAACGCCACACTCTCCCAA
PcoLac2_ rnai_fw	*TAATACGACTCACTATAGGG*ACGGCAAAGGACAATTCAGG
PcoLac2_ rnai_rev	*TAATACGACTCACTATAGGG*AGGCCTGGGTTGCAAAATTC
CpopTH_ rnai_fw	*TAATACGACTCACTATAGGG*TCAACGCGCAGTATTGGTCT
CpopTH_ rnai_rev	*TAATACGACTCACTATAGGG*GAACACCTTGCGGTACTCCA
PcoTH_ rnai_fw	*TAATACGACTCACTATAGGG*ACAAGGAATACCGTGCCAGG
PcoTH_rnai_rev	*TAATACGACTCACTATAGGG*CCGAACTCGACAGTGAACCA
RNA FISH:	
CpopGR1_fish_fw	ATGTTCACTCGGATATTGGCGTT
CpopGR1_fish_rev	TCAGTTCCTAGGTATCTTCTGTATGTGA
CpopOBP13_fish_fw	ATGTCTCCTTACAGTGCCAGTCCTGCAT
CpopOBP13_fish_rev	TTAAACAAGGCTGAGATGTGAGGGGG
CpopActin_fish_fw	ATGTGTGACGATGATGTAGCGGC
CpopActin_fish_rev	TTAGAAGCACTTGCGGTGGACG